Impedance Modeling of Electromagnetic Energy Harvesting System Using Full-Wave Bridge Rectifier

Junrui Liang[a], Cong Ge[a], and Yi-Chung Shu[b]

[a]School of Information Science and Technology, ShanghaiTech University, Shanghai, China
[b]Institute of Applied Mechanics, National Taiwan University, Taipei 106, Taiwan

ABSTRACT

In the conventional model of general vibration energy harvesters, the harvesting effect was regarded as only the electrically induced damping. Such intuition has overlooked the detailed dynamic contribution of practical power conditioning circuits. This paper presents an improved impedance model for the electromagnetic energy harvesting (EMEH) system considering the detailed dynamic components, which are introduced by the most extensively used full-wave bridge rectifier. The operation of the power electronics is studied under harmonic excitation. The waveforms, energy cycles, and impedance picture are illustrated for showing more information about the EMEH system. The theoretical prediction on harvesting power can properly describe the changing trend of the experimental result.

Keywords: Electromagnetic, energy harvesting, impedance analysis, electromechanical joint dynamics

1. INTRODUCTION

The kinetic energy harvesting, as one of the important energy harvesting technologies, has been extensively investigated nowadays. With these technologies, future distributed and wearable electronics, which are exposed to mechanical vibrations, can become self-powered by scavenging energy from the ambient vibration sources. The electromechanical transducers play an important role in the energy harvesting systems. The electromagnetic (EM) and piezoelectric (PE) ones are two of the most studied transducers towards the implementation of energy harvesting systems in both macro and micro scales.

The electromagnetic energy harvester generates electricity according to the Faraday's law of induction, which is very classical. Yet, the introduction of nonlinear power conditioning circuit, which is necessary for the ac-to-dc power conversion, as the targeted application is mostly digital electronics, has brought in some new problems for the investigation of the *electromechanical joint dynamics*. The same problem also exists for other kinetic energy harvesting systems, such as piezoelectric, electrostatic, etc. Most of the previous studies take the effect of energy harvesting as the *electrically induced damping*,[1–4] regardless of different types of the transducers and connected circuits. Intuitively speaking, it is quite straightforward, because removing energy from a vibrating system will certainly damp the vibration. Yet, when looking into the details, the coupling features of different transducers are different; the harvesting performances of different power conditioning circuits are different too. Therefore, the electrically induced damping equivalent is more appropriate to be referred to as the *nominal* or *ideal* model of a vibration energy harvester. The implementations of energy harvesting systems with practical ac-to-dc rectification have more detailed dynamic contents in addition to merely the electrically induced damping.

The difficulty of the joint dynamic modeling lies on that the mechanical dynamics are usually described with ordinary differential equations (ODEs) for lumped structures, or partial differential equations (PDEs) for parameter distributed structures; while the electrical power conditioning circuits are nonlinear. When both parts are connected together, mathematically speaking, the expression of the joint dynamics and the harvested power are the steady-state solutions of the *nonlinear differential equations*. Numerical methods or tools are usually taken for deriving the steady-state behavior. These methods can be derived from time domain[5] or frequency domain.[6–9]

Corresponding author: Junrui Liang. E-mail: liangjr@shanghaitech.edu.cn.
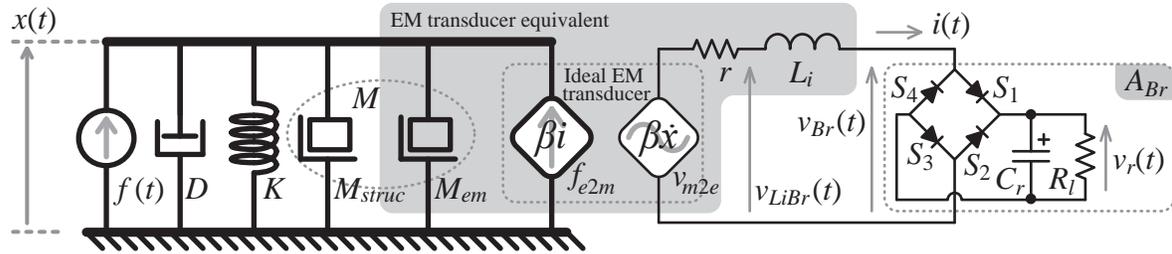
Figure 1. Schematics of an EMEH system using full-wave bridge rectifier.

This paper proposes a joint dynamic model of an electromagnetic energy harvesting (EMEH) system using full-wave bridge rectifier by describing the dynamics of both mechanical and electrical parts in a common "language", the *equivalent impedance*. By taking this method, the dynamic details with practical energy harvesting circuits can be better revealed and understood.

2. SYSTEM CONFIGURATION

An EMEH system is composed of three major parts: the *mechanical structure* delivering kinetic energy from the vibration source to the transducer; the *EM transducer* transforming the mechanical energy into electrical form; and the *power conditioning circuit*, which is also referred to as the *interface circuit*, carrying out ac-to-dc conversion for the digital electronic end devices.

2.1 EM Transducer

The transducer is a key component enabling the electromechanical power transformation. We start from the two-port network of an ideal EM transducer. According to the Lorentz force law and Faraday's law of induction, when an EM harvester is moving within a small range, in which the magnetic field intensity can be regarded as homogeneous, the constitutive relation of an ideal electromagnetic transducer is described by the following linear equations:[5]

$$\begin{cases} f_{e2m}(t) = \beta i(t); \\ v_{m2e}(t) = \beta \dot{x}(t), \end{cases} \tag{1}$$

where β is the electromechanical coupling factor; x is the vibration displacement, whose derivative $\dot{x}$ is the velocity; v_{m2e} is the mechanical motion induced electromotive force (EMF); i is current flowing through the transducer; f_{e2m} denotes the charge movement induced Lorentz force acting on the current-carrying wire.

2.2 EMEH System

The EMEH system can be broken down into the schematics shown Figure 1 by importing the ideal EM transducer model, and figuring out other dynamic components. In the schematics, $f(t)$ is the external force source; D, K, and M_{struc} are the damping coefficient, stiffness, and mass of the mechanical main structure, respectively; f_{e2m} and v_{m2e} form the ideal EM transducer. M_{em} models the mass of the moving part of the EM transducer, which is combined with M_{struc} into a total mass $M = M_{struc} + M_{em}$ (M will be used in later discussion). L_i represents the self-inductance of the electromagnetic coil; r is the equivalent series resistance (ESR) of the coil. In the circuit part, the diodes S_1 to S_4 form a bridge rectifier; C_r is the filter capacitor and also the dc storage; R_l is the load resistor.

Based on the breakdown schematics shown in Figure 1, we can write the system-level constitutive equations for the EMEH system in the time domain, which mathematically summarizes the parallel mechanical connection and series electrical connection as follows

$$\begin{cases} f(t) = M\ddot{x}(t) + D\dot{x}(t) + Kx(t) + \beta i(t); \\ \beta\dot{x}(t) = ri(t) + L_i\dot{i}(t) + A_{Br}\left[i(t)\right]. \end{cases} \tag{2}$$

The rectified circuit is a nonlinear module, in fact. But for constructing the equivalent impedance model, whose conventional concept is linear, we have to assume that the dynamic behavior of the ac-to-dc rectified circuit (a full-wave bridge rectified here) can be substituted by its linear equivalent, which approximately maps $i(t)$ into $v_{Br}(t)$. Such dynamics is summarized by a equivalent linear operator A_{Br}, as shown in Figure 1 and used in (2).

3. IMPEDANCE MODELING

The concept of impedance expresses the dynamics of a component or a dynamic network in the frequency domain as the ratio of complex phasors of the effort to flow variables.[5] The conventional impedance concept can be only applied to linear time-invariant (LTI) system. A linear approximation based on harmonic analysis is adopted for transplanting this modeling methodology to the analysis of piezoelectric energy harvesting (PEEH)[6] and EMEH systems in this study.

3.1 System Dynamics in a Single Equation

The time-domain system-level constitutive equations provided in (2) connect the mechanical and electrical domains. For more clearly showing the joint dynamics, we have to combine both equations into a single equation, express the dynamics in either fully mechanical aspect or fully electrical aspect.

Converting (2) into frequency domain and eliminating the current $i(t)$ by substituting the second equation into the first, we can have

$$\frac{F(s)}{sX(s)} = \Sigma\hat{Z}(s) = sM + D + \frac{K}{s} + \frac{\beta^2}{r + sL_i + \check{Z}_{Br}(s)}. \tag{3}$$

We regard the last fractional item in (3) as the equivalent mechanical impedance resulting from the total electrical dynamics $\Sigma\check{Z}(s)$, i.e.,

$$\hat{Z}_{e2m}(s) = \frac{\beta^2}{r + sL_i + \check{Z}_{Br}(s)} = \frac{\beta^2}{\Sigma\check{Z}(s)}. \tag{4}$$

To distinguish the dynamics from either mechanical or electrical point of view, the variables with hat symbol, i.e., $\hat{Z}$ and $\hat{Y}$ denote the mechanical impedance and admittance; while those with check symbol, i.e., $\check{Z}$ and $\check{Y}$ denote the electrical ones. In (4), $\check{Z}_{Br}(s)$ is the frequency-domain correspondence of the linear operator A_{Br} in (2). They are linked by the Laplace transformation, i.e., $\check{Z}_{Br}(s) = \mathscr{L}[A_{Br}]$. On the other hand, as a nonlinear circuit, the voltage and current relation of a bridge rectifier is unable to be separately considered without combining with the source impedance of the transducer, as indicated in the previous PEEH study.[10] Therefore, in this EMEH study, the dynamic effect produced by the combination of self-inductance L_i and bridge rectifier A_{Br} is considered as a whole, i.e.,

$$\check{Z}_{LiBr}(s) = sL_i + \check{Z}_{Br}(s) \tag{5}$$

from the electrical aspect, or

$$\hat{Z}_{LiBr}(s) = \frac{\beta^2}{\check{Z}_{LiBr}(s)} \tag{6}$$

from the mechanical aspect.

The bridge rectifier is simply taken as a voltage controlled switch in this model. In the PEEH case, by taking the rectifier circuit and the parallel connected source capacitance as a whole, the voltage can be formulated as a piecewise integral of the current. In this EMEH case, by taking the rectifier and the series connected source inductance as a whole, accordingly, the current can be formulated as a piecewise integral of the voltage. However, more generally speaking, besides the self-inductance L_i, there is an ESR r in the EM transducer source, as viewed from the electrical port. The reason why excluding r in the combination is for reducing the modeling complexity. Otherwise, we need to solve a *piecewise integral equation* to describe the voltage and current relation for the r, L_i, and A_{Br} combination. It will be much more troublesome than merely doing *piecewise integral*. Therefore, the ESR r is taken as an individual component in the impedance network in series with $\check{Z}_{LiBr}(s)$. Such modeling technique was also used for considering the effect of dielectric loss in the PEEH systems.[8]

3.2 Operation Modes and Equivalent Admittance $\check{Y}_{LiBr}$

For deriving the equivalent impedance of the self-inductance and bridge rectifier combination $\check{Z}_{LiBr}$, it is first assumed that its input voltage v_{LiBr}, as illustrated in Figure 1, is pure sinusoidal, i.e.,

$$v_{LiBr}(t) = V_{LiBr}\sin(\omega t), \tag{7}$$

where V_{LiBr} is the magnitude; ω is the vibration angular frequency. As C_r is designed for the filtering purpose, it is usually selected as large as that v_r, the voltage across C_r, seems a constant voltage V_r. In other words, we design C_r such that the self-inductance dominates the current and voltage relation when the bridge rectifier is conducted, i.e.,

$$\frac{1}{\omega C_r} \ll \omega L. \tag{8}$$

As a diode can be simply taken as a unidirectional electronic switch with a specific threshold voltage, which can be either on or off, the operation of the power conditioning circuit in each cycle can be divided into a few states. In the PEEH system, given the parallel piezoelectric capacitance, which is driven by the harmonic current source, it is quite straightforward to write out the piecewise voltage equation.[6] In the EMEH system, there is a series inductance connected to the bridge rectifier, the conduction state of the bridge rectifier is decided by both v_{LiBr} and the voltage across the inductance. When driven by an harmonic voltage v_{LiBr}, the current flowing through L_i and the bridge rectifier can be generally divided into four operational states: forward conduction (S_1 and S_3 are on), reverse conduction (S_2 and S_4 are on), and two blocked states (all diodes are off) in between the two conduction states. The current $i(t)$ can be expressed with the piecewise equation as follows

$$i(t) = \frac{V_{LiBr}}{\omega L_i} \times \begin{cases} -\cos\theta - \tilde{V}_{Br}\theta \Big|_{\theta=2k\pi+\theta_0}^{\omega t}, & 2k\pi + \theta_0 \le \omega t < 2k\pi + \theta_1; \\ 0, & 2k\pi + \theta_1 \le \omega t < 2k\pi + \pi + \theta_0; \\ -\cos\theta + \tilde{V}_{Br}\theta \Big|_{\theta=2k\pi+\pi+\theta_0}^{\omega t}, & 2k\pi + \pi + \theta_0 \le \omega t < 2k\pi + \pi + \theta_1; \\ 0, & 2k\pi + \pi + \theta_1 \le \omega t < 2k\pi + 2\pi + \theta_0; \end{cases} \tag{9}$$

where

$$\tilde{V}_{Br} = \frac{V_{Br}}{V_{LiBr}} = \frac{V_r + V_F}{V_{LiBr}} \tag{10}$$

is the normalized rectified voltage. V_F is the forward voltage drop across the bridge rectifier.

In (9), θ_0 and θ_1 are unknowns to be determined under different current conduction modes. If the bridge rectifier is blocked, i.e., current through the L_i becomes zero, before $|v_{LiBr}| \ge V_{Br}$, the circuit operates under the discontinuous-conduction mode (DCM); otherwise, it operates under the continuous-conduction mode (CCM). Because the inductance current cannot suddenly change, the current in between the forward conduction (positive current) and reverse conduction (negative current) must be zero. Therefore, no matter the circuit works under DCM or CCM, each conduction phase starts from zero current and ends with zero current as well. Regarding to the zero current change after every conduction phase, i.e., $i(\theta_1/\omega) = i(\theta_0/\omega) = 0$, from (9), we have

$$\cos\theta_1 - \cos\theta_0 + \tilde{V}_{Br}(\theta_1 - \theta_0) = 0. \tag{11}$$

In CCM, the forward and reverse conduction phases make a nose-to-tail connection, i.e., there is no second and fourth zero-current states in (9); therefore we have

$$\theta_{1,ccm} = \theta_{0,ccm} + \pi. \tag{12}$$

Substituting the CCM phase relation in (12) into the general relation provided in (11) and solving the equation, we can get the conduction start phase in CCM expressed as follows

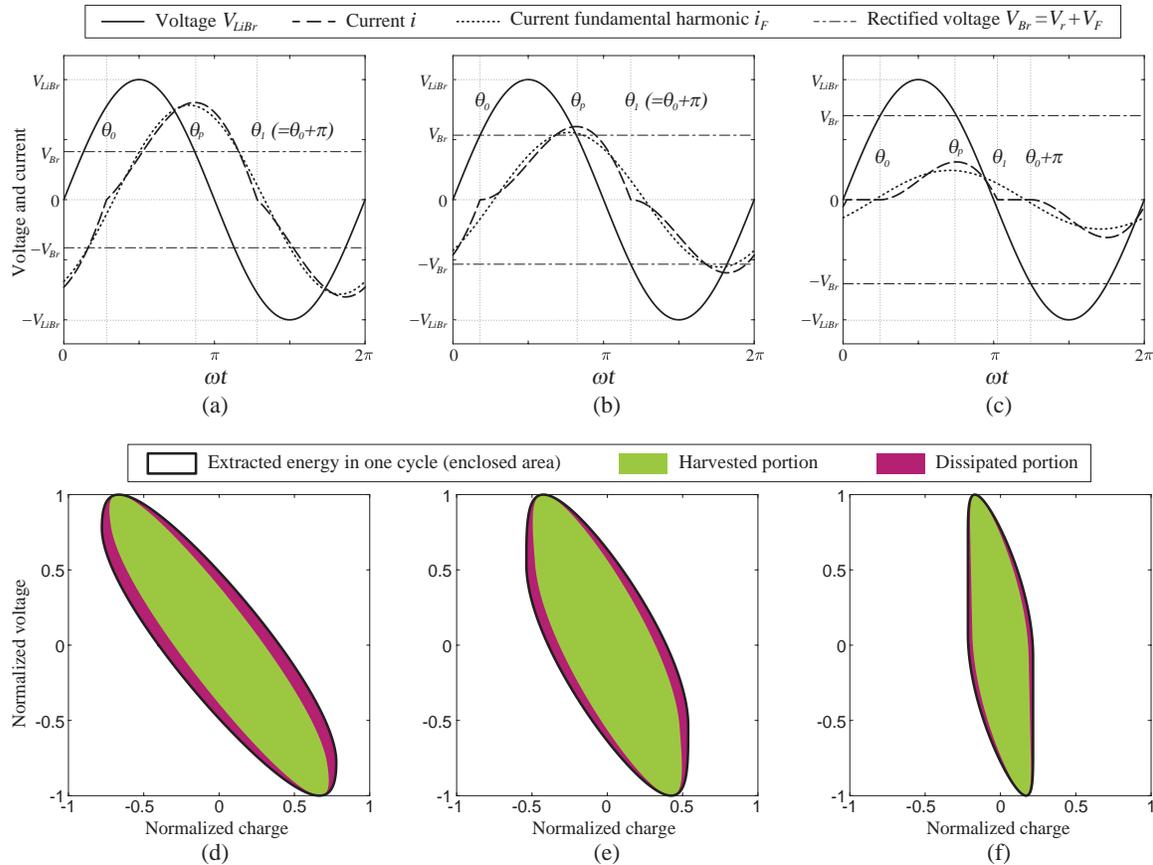$$\theta_{0,ccm} = \cos^{-1}\frac{\pi\tilde{V}_{Br}}{2}. \tag{13}$$

Figure 2. Voltage and current waveforms and work cycles (charge-voltage diagrams) in EMEH with bridge rectifier ($\tilde{V}_F = 0.1$). (a) Waveforms under CCM. (b) Waveforms at the critical point. (c) Waveforms under DCM. (d) Work cycle under CCM. (b) Work cycle under at the critical point. (c) Work cycle under DCM.

The voltage and current waveforms as well as the work cycle, i.e., the charge-voltage diagram, under CCM are illustrated in Figure 2(a) and (d). Figure 2(a) is obtained according to the charge, i.e., integration of (9) and the voltage given by (7). The enclosed area in Figure 2(d) represents the extracted energy in each cycle, while the green and purple ones represent the harvested and dissipated portions within the extraction. Since the same amount charge flows through the series voltages V_F and V_r, the voltage across the filter capacitor C_r, during the conduction, the ratio of dissipated power and harvested power is just V_F/V_r. Figure 2(d) is obtained under the normalized rectifier forward voltage drop $\tilde{V}_F = 0.1$, whose definition is given by

$$\tilde{V}_F = \frac{V_F}{V_{LiBr}}. \tag{14}$$

In DCM, the conduction starts when $v_{LiBr}(t) = V_{Br}$, therefore we have

$$\theta_{0,dcm} = \sin^{-1} \tilde{V}_{Br}. \tag{15}$$

Combining the DCM specific condition (15) and the general condition (11), the conduction end phase in DCM, i.e., $\theta_{1,dcm}$, can be obtained *implicitly* by solving the transcendental equations set. The voltage and current waveforms as well as the work cycle, i.e., the charge-voltage diagram under DCM, are illustrated in Figure 2(c) and (f). It can be observed from Figure 2(c) that the current between θ_1 and $\theta_0 + \pi$ is zero. The bridge rectifier is blocked during this time slot. In DCM, the dissipated portion has a smaller percentage in the extracted energy, because, given the increase of V_r and constant V_F, the ratio V_F/V_r is smaller compared to the CCM case.
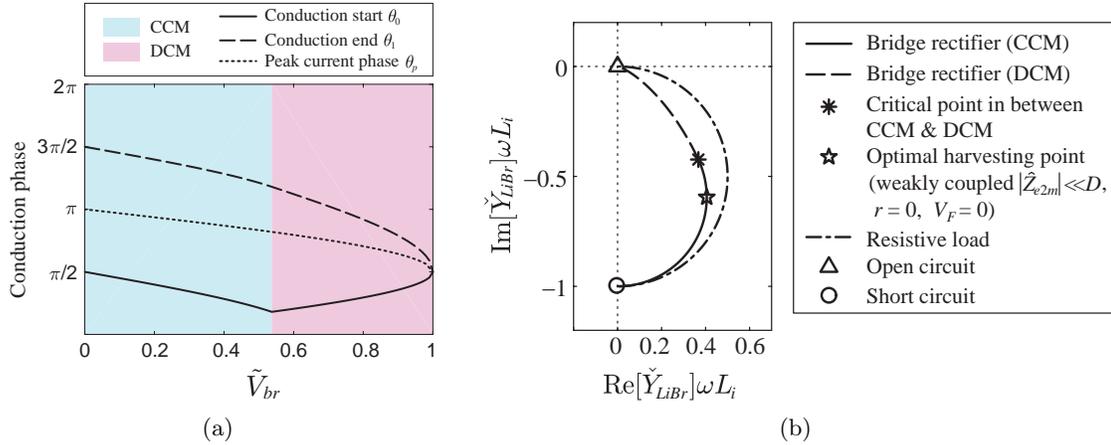
Figure 3. The switching phases and equivalent admittances in EMEH with bridge rectifier. (a) The switching start, end, and peak current phases in CCM and DCM. (c) Equivalent admittance.

There is a critical point connecting CCM and DCM, in which all (11), (12), and (15) hold. Solving the equations set, which is combined with (11), (12), and (15) (three equations with three unknowns), gives the critical voltage ratio $\tilde{V}_{Br,cr}$ as follows

$$\tilde{V}_{Br,cr} = \frac{2}{\sqrt{4 + \pi^2}} \approx 0.5370. \tag{16}$$

At the critical operation, the conduction start and end phases can be specified as follows

$$\begin{cases} \theta_{0,cr} = \tan^{-1} \dfrac{2}{\pi}; \\ \theta_{1,cr} = \theta_{0,cr} + \pi. \end{cases} \tag{17}$$

The voltage and current waveforms as well as the work cycle, i.e., the charge-voltage diagram, at the critical condition are illustrated in Figure 2(b) and (e). Figure 3(a) shows the overall picture of the conduction start phase θ_0, conduction end phase θ_1, and peak current phase θ_p as functions of the normalized rectified voltage $\tilde{V}_{Br}$, where the result of the DCM part is numerically obtained by solving the transcendental equations. By knowing about these conduction start and end angles, the current $i(t)$ flowing through $\check{Y}_{LiBr}$, the combination of L_i and the bridge rectifier, therefore, can be drawn according to (9), as shown in Figure 2(a)-(c). The fundamental harmonic of $i(t)$, which is denoted as $i_F(t)$, under different cases are also numerically obtained and shown in Figure 2(a)-(c). Base on the frequency-domain counterparts of sinusoidal voltage $v_{LiBr}(t)$ and the current fundamental harmonic $i_F(t)$, we can follow the similar formula, which was used in the PEEH study,[6] and obtain the expression of electrical equivalent admittance as follows

$$\check{Y}_{LiBr}(s) = \frac{I_F(s)}{V_{LiBr}(s)}. \tag{18}$$

We choose admittance here to describe the dynamics of the L_i and bridge rectifier combination, rather than impedance as that used in the PEEH case, because of the series connection of two compositions. In EMEH, as the rectified voltage $\tilde{V}_{Br}$ goes up, the admittance moves from a finite place to zero, rather than to infinity as its impedance does. The full admittance picture is easier to be shown in the complex plane. Figure 3(b) shows the picture of $\check{Y}_{LiBr}$. By changing the rectified voltage V_{Br} from zero to V_{LiBr}, the equivalent admittance $\check{Y}_{LiBr}$ moves along the specific curve from the short-circuited point (circular marker) to the open-circuited point (triangular marker). The CCM segment is illustrated with solid line, while the DCM segment is illustrated with dashed line. For comparison, the admittance of self-inductance L_i with resistive load (replacing the bridge rectifier) is also shown in Figure 3(b). The L_i and resistive load combination gives the admittance in a semicircle. It can be observed from Figure 3(b) that, the two loading conditions crossover only at the open-circuited and short-circuited points, which means, strictly speaking, the resistive load cannot represent the dynamics of the bridge rectifier circuit. Similar conclusion was also drawn in the PEEH study.[6]
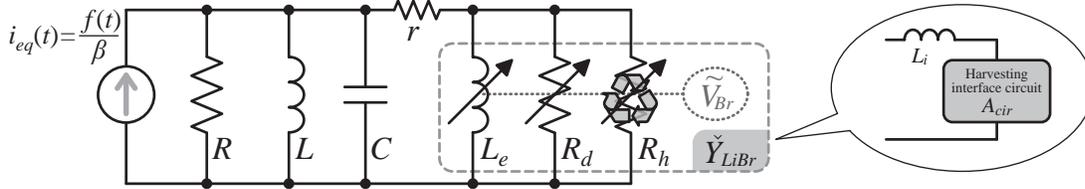
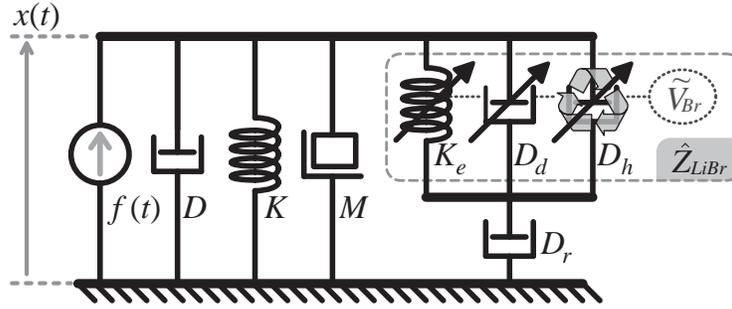Figure 4. Equivalent impedance network of the EMEH system.

Figure 5. Equivalent mechanical schematics of the EMEH system.

3.3 Detailed Dynamic Components in $\check{Y}_{LiBr}$

From the admittance picture of $\check{Y}_{LiBr}$, which was shown in Figure 3(b), the overall dynamics of the self-inductance and bridge rectifier combination is still inductive, because the imaginary part of the admittance is negative. The imaginary part, i.e., the effective susceptance B_e, which providing the reactive power, can be singled out as one of the detailed dynamic components in $\check{Y}_{LiBr}$. On the other hand, considering the forward voltage drop of the bridge rectifier, the extracted power can be divided into two portions, the harvested power and dissipated power. Those concept on energy flow was explained in details in the PEEH study.[6,11] Therefore, the real part of $\check{Y}_{LiBr}$ can be further divided into the harvested and dissipated components, which are denoted as G_h and G_d, respectively. The ratio $G_h/G_d = V_r/V_F$. In general, the dynamic effect of $\check{Y}_{LiBr}$ can be broken down into three detailed components connected in parallel, i.e.,

$$\check{Y}_{LiBr}(s) = G_h + G_d + jB_e = \frac{1}{R_h} + \frac{1}{R_d} + \frac{1}{sL_e}. \tag{19}$$

The actual values of the three components are functions of the normalized rectified voltage $\tilde{V}_{Br}$, as different $\tilde{V}_{Br}$ changes the current waveforms, as shown in Figure 2.

To consider the harvested power in practical EMEH system, we should rely on the system level model. For example, describing the joint dynamics of the entire EMEH system in an *equivalent electrical impedance network*. Such a network can be formulated by substituting (19) and (5) into (3) and doing some variable substitutions, as follows

$$\check{Z}_{EMEH}(s) = \frac{V_{m2e}(s)}{I_{eq}(s)} = \frac{1}{sC} \parallel R \parallel sL \parallel (r + R_h \parallel R_d \parallel sL_e), \tag{20}$$

In (20), the symbol '$\parallel$' defines the operation $Z_1 \parallel Z_2 \triangleq (Z_1^{-1} + Z_2^{-1})^{-1}$, which has a higher operational priority over the addition '+' operation. The equivalent variables $V_{m2e}(s)$, $I_{eq}(s)$ and equivalent components C, R, L are obtained from the mechanical domain with the following electromechanical analogy

$$V_{m2e}(s) = \beta sX(s); \quad I_{eq}(s) = \frac{F(s)}{\beta}; \quad C = \frac{M}{\beta^2}; \quad R = \frac{\beta^2}{D}; \quad L = \frac{\beta^2}{K}. \tag{21}$$

The equivalent electrical impedance network given in (20) is also graphically illustrated in Figure 4. Similar to the denotations in the equivalent impedance network of PEEH system,[6] the arrows on R_h, R_d, and L_e in the network denote the variations of these three dynamic components, which are functions of the rectified voltage
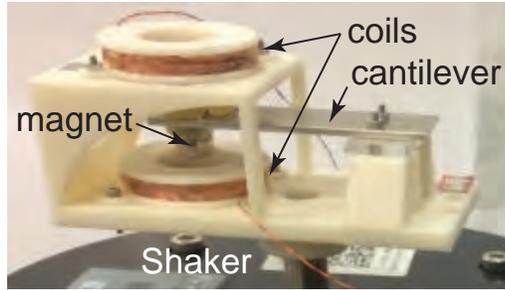
Figure 6. Experimental setup.

Component	Identified Value	Experimental Condition	Value
R	216.58 Ω	Base acceleration $\ddot{Y}$	1.5 g
L	4.042 mH	V_{oc} under $\ddot{Y}$	6 V
C	0.32 mF	Operating frequency f	139 Hz
L_i	272.62 mH	Rectifier voltage drop V_F	0.47 V
r	839.20 Ω		
β	1.70 N/A		

Table 1. Identified parameters and experimental conditions.

$\tilde{V}_{Br}$. The functional dependency is denoted by the dashed link to $\tilde{V}_{Br}$ in both Figure 4. The harvested power P_h corresponds to the power absorbed by the harvesting component R_h during steady-state operation.

Beside the equivalent electrical impedance network, which is more favorable by electrical engineers, the electromechanical joint dynamics can also be presented in the equivalent mechanical schematics for mechanical engineers, as shown in Figure 5. The equivalent mechanical impedance of the entire system can be also derived from (3), as follows

$$\hat{Z}_{EMEH}(s) = \frac{F(s)}{sX(s)} = sM + D + \frac{K}{s} + D_r \parallel \left(D_h + D_d + \frac{K_e}{s} \right), \tag{22}$$

where the equivalent components D_r, D_h, D_d, and K_e are obtained from the electrical domain with the following electromechanical analogy

$$D_r = \frac{\beta^2}{r}; \quad D_h = \frac{\beta^2}{R_h}; \quad D_d = \frac{\beta^2}{R_d}; \quad K_e = \frac{\beta^2}{L_e}. \tag{23}$$

The electromechanical analogy shown in (21) and (23) is different from that in the PEEH study.[6,8] The equivalent electrical impedance network in the PEEH and EMEH cases are different as well. Yet, from the mechanical point of view, both of the PEEH and EMEH systems derive the same equivalent mechanical schematics.[8]

4. EXPERIMENT

An experiment is carried out for validating the impedance based model towards the analysis of electromechanical joint dynamics and the evaluation of harvested power for the EMEH systems. The experimental setup is shown in Figure 6. The electromechanical transducer is composed of a permanent magnet as the moving part, which is mounted at the free end of a base excited cantilever, and two coils fixed at the base around the magnetic poles. The two coils are connected in series for increasing the output voltage.

Before connecting to the power conditioning circuit, by looking into the two electrodes of the EM coil, the dynamics of the open-circuited EM structure can be specified as

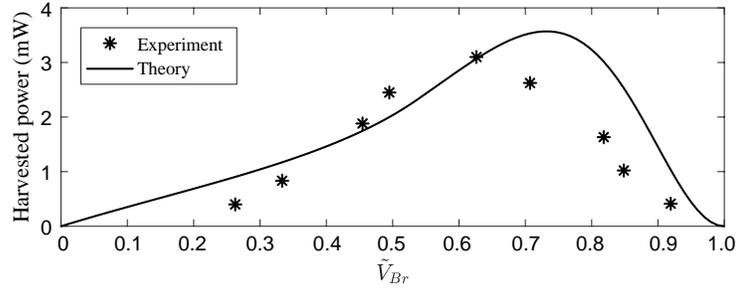$$\check{Z}_{in} = r + sLi + \left(R \parallel sL \parallel \frac{1}{sC} \right). \tag{24}$$
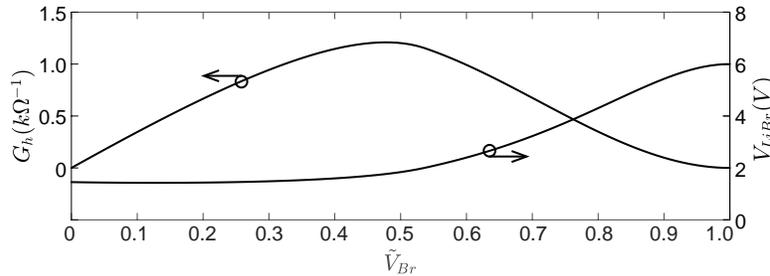
Figure 7. The result of harvested power.

Figure 8. The functional relation between phase difference and the normalized rectified voltage.

$\check{Z}_{in}$ of the experimental EM structure is measured with an impedance analyzer. By fitting the measurement data, we can identify the five component values in (24). Those values as well as some experimental conditions are listed in Table 1.

With those identified parameters, we are able to generate the theoretical picture about the harvested power according to the systematic equivalent impedance network, which was formulated in (20) and the equation about resistive heating as follows

$$P_{h,theory} = \frac{V_{LiBr}^2 G_h}{2} = \frac{V_{LiBr}^2}{2R_h}. \tag{25}$$

In experiment, we maintain the magnitude of the base acceleration, record the change of V_r under different dc load resistance R_l. Therefore, the experimental result of harvested power can be obtained as follows

$$P_{h,experiment} = \frac{V_r^2}{R_l}. \tag{26}$$

The theoretical and experimental results are compared in Figure 7. It shows that the theory can basically predict the amount as well as the changing trend of the harvested power in the studied EMEH system. However, there do have a little discrepancy on the peak places of the two results. Future work will focus on the refinements of the theoretical derivation and the experimental conditions towards more accurate model and validation.

From the results of harvested power, no matter for the theoretical or experimental one, we can observed that the peak harvested power actually locates at the right-half plane, i.e., the DCM region, rather than the CCM region as illustrated in Figure 3(b). By plotting out the V_{LiBr} and G_h, which are related to the harvested power, as functions of $\tilde{V}_{Br}$ in Figure 8, we find that G_h actually peaks at the CCM region; yet, V_{LiBr} is quite small in this CCM region. The reason is because the ESR in an air coil is quite large compared to the impedance magnitude of the coil inductance; therefore, it dominates the dynamics in most of the CCM region given their series connection. In order to move the harvested power peak towards the more efficient CCM region, the design of induction coil in the EM device needs more detailed investigation based on the theoretical guidance.

5. CONCLUSION

The electromagnetic energy harvesting (EMEH) system converts the vibration power into electricity based on the extensively used magnetic induction principle. Yet, even the EM transducer is classical and well understood, the

introduction of nonlinear ac-to-dc power conditioning circuit has brought new problems to the studies of EMEH systems. The electromechanical joint dynamics is of concern, given its synergistic design and optimization in both mechanical and electrical sides. This paper has shown the possibility of studying the joint dynamics based on a common "language" of both sides, the *equivalent impedance*. The observations on the harvested power results give some hints towards more efficient design and possible improvement in future studies.

ACKNOWLEDGMENTS

REFERENCES

[1] Williams, C. B. and Yates, R. B., "Analysis of a micro-electric generator for microsystems," *Sens. Actuators, A* **52**(1–3), 8–11 (1996).

[2] Beeby, S. P., Tudor, M. J., and White, N. M., "Energy harvesting vibration sources for microsystems applications," *Meas. Sci. Technol.* **17**(12), R175–R195 (2006).

[3] Cook-Chennault, K. A., Thambi, N., and Sastry, A. M., "Powering MEMS portable devices – a review of non-regenerative and regenerative power supply systems with special emphasis on piezoelectric energy harvesting systems," *Smart Mater. Struct.* **17**(4), 043001 (2008).

[4] Khaligh, A., Zeng, P., and Zheng, C., "Kinetic energy harvesting using piezoelectric and electromagnetic technologies – state of the art," *IEEE Trans. Ind. Electron.* **57**, 850–860 (March 2010).

[5] Cheng, S., Wang, N., and Arnold, D. P., "Modeling of magnetic vibrational energy harvesters using equivalent circuit representations," *J. Micromech. Microeng.* **17**(11), 2328–2335 (2007).

[6] Liang, J. R. and Liao, W. H., "Impedance modeling and analysis for piezoelectric energy harvesting systems," *IEEE/ASME Trans. Mechatron.* **17**(6), 1145–1157 (2012).

[7] Lien, I. C. and Shu, Y. C., "Array of piezoelectric energy harvesting by the equivalent impedance approach," *Smart Mater. Struct.* **21**(8), 082001 (2012).

[8] Liang, J. R., Chung, H. S.-H., and Liao, W.-H., "Dielectric loss against piezoelectric power harvesting," *Smart Mater. Struct.* **23**(9), 092001 (2014).

[9] Wu, P. and Shu, Y., "Finite element modeling of electrically rectified piezoelectric energy harvesters," *Smart Materials and Structures* **24**(9), 094008 (2015).

[10] Liang, J. R. and Liao, W. H., "Piezoelectric energy harvesting and dissipation on structural damping," *J. Intell. Mater. Syst. Struct.* **20**(5), 515–527 (2009).

[11] Liang, J. R. and Liao, W. H., "Energy flow in piezoelectric energy harvesting systems," *Smart Mater. Struct.* **20**(1), 015005 (2011).